

Ginzburg-Landau theory of vortices in a multi-gap superconductor

M. E. Zhitomirsky and V.-H. Dao

Commissariat à l'Energie Atomique, DMS/DRFMC/SPSMS,
17 avenue des Martyrs, 38054 Grenoble, Cedex 9 France

(Dated: September 14, 2018)

The Ginzburg-Landau functional for a two-gap superconductor is derived within the weak-coupling BCS model. The two-gap Ginzburg-Landau theory is, then, applied to investigate various magnetic properties of MgB₂ including an upturn temperature dependence of the transverse upper critical field and a core structure of an isolated vortex. Orientation of vortex lattice relative to crystallographic axes is studied for magnetic fields parallel to the *c*-axis. A peculiar 30°-rotation of the vortex lattice with increasing strength of an applied field observed by neutron scattering is attributed to the multi-gap nature of superconductivity in MgB₂.

PACS numbers: 74.70.Ad, 74.20.De, 74.25.Qt

I. INTRODUCTION

Superconductivity in MgB₂ discovered a few years ago¹ has attracted a lot of interest both from fundamental and technological points of view.² Unique physical properties of MgB₂ include $T_c = 39$ K, the highest among *s*-wave phonon mediated superconductors, and the presence of two gaps $\Delta_1 \approx 7$ meV and $\Delta_2 \approx 2.5$ meV evidenced by the scanning tunneling^{3,4} and the point contact^{5,6} spectroscopies and by the heat capacity measurements.^{7,8,9,10} The latter property brings back the concept of a multi-gap superconductivity^{11,12} formulated more than forty years ago for materials with large disparity of the electron-phonon interaction for different pieces of the Fermi surface.

Theoretical understanding of normal and superconducting properties of MgB₂ has been advanced in the direction of first-principle calculations of the electronic band structure and the electron-phonon interaction, which identified two distinct groups of bands with large and small superconducting gaps.^{13,14,15,16,17,18,19} Quantitative analysis of various thermodynamic and transport properties in the superconducting state of MgB₂ was made in the framework of the two-band BCS model.^{20,21,22,23,24,25,26,27,28} An outside observer would notice, however, a certain lack of effective Ginzburg-Landau or London type theories applied to MgB₂. This fact is explained by quantitative essence of the discussed problems, though effective theories can often give a simpler insight. Besides, new experiments constantly raise different types of questions. For example, recent neutron diffraction study in the mixed state of MgB₂ has found a strange 30°-reorientation of the vortex lattice with increasing strength of a magnetic field applied along the *c*-axis.²⁹ Such a transition represents a marked qualitative departure from the well-known behavior of the Abrikosov vortex lattice in single-gap type-II superconductors. Nature and origin of phase transitions in the vortex lattice are most straightforwardly addressed by the Ginzburg-Landau theory.

In the present work we first derive the appropriate Ginzburg-Landau functional for a two-gap superconduc-

tor from the microscopic BCS model. We, then, investigate various magnetic properties of MgB₂ using the Ginzburg-Landau theory. Our main results include demonstration of the upward curvature of $H_{c2}(T)$ for transverse magnetic fields, investigation of the vortex core structure, and explanation of the reorientational transition in the vortex lattice. The paper is organized as follows. Section 2 describes the two-band BCS model and discusses the fit of experimental data on the temperature dependence of the specific heat. Section 3 is devoted to derivation of the Ginzburg-Landau functional for a two-gap weak-coupling superconductor. In Section 4 we discuss various magnetic properties including the upper critical field and the structure of an isolated vortex. Section 5 considers the general problem of an orientation of the vortex lattice in a hexagonal superconductor in magnetic field applied parallel to the *c*-axis and, then, demonstrates how the multi-gap nature of superconductivity in MgB₂ determines a reorientational transition in the mixed state.

II. THE TWO-BAND BCS MODEL

A. General theory

In this subsection we briefly summarize the thermodynamics of an *s*-wave two-gap superconductor with the aim to extract subsequently microscopic parameters of the model from available experimental data for MgB₂. We write the pairing interaction as

$$\hat{V}_{\text{BCS}} = - \sum_{n,n'} g_{nn'} \int dx \Psi_{n\uparrow}^\dagger(x) \Psi_{n\downarrow}^\dagger(x) \Psi_{n'\downarrow}(x) \Psi_{n'\uparrow}(x) , \quad (1)$$

where $n = 1, 2$ is the band index. A real space representation (1) is obtained from a general momentum-space form of the model^{11,12} under assumption of weak momentum dependence of the scattering amplitudes $g_{nn'}$. We also assume that the active band has the strongest pairing interaction $g_{11} = g_1$ compared to interaction in the passive band $g_{22} = g_2$ and to interband scattering

of the Cooper pairs $g_{12} = g_{21} = g_3$. Defining two gap functions

$$\Delta_n(x) = - \sum_{n'} g_{nn'} \langle \Psi_{n'\downarrow}(x) \Psi_{n'\uparrow}(x) \rangle \quad (2)$$

the total Hamiltonian is transformed to the mean-field form

$$\hat{H}_{\text{MF}} = E_{\text{const}} + \sum_n \int dx \left[\Psi_{n\sigma}^\dagger(x) \hat{h}(x) \Psi_{n\sigma}(x) + \Delta_n(x) \Psi_{n\uparrow}^\dagger(x) \Psi_{n\downarrow}^\dagger(x) + h.c. \right], \quad (3)$$

$\hat{h}(x)$ being a single-particle Hamiltonian of the normal metal. The constant term is a quadratic form of anomalous averages $\langle \Psi_{n\downarrow}(x) \Psi_{n\uparrow}(x) \rangle$. Using Eq. (2) it can be expressed via the gap functions

$$E_{\text{const}} = \frac{1}{G} \int dx [g_2 |\Delta_1|^2 + g_1 |\Delta_2|^2 - g_3 (\Delta_1^* \Delta_2 + \Delta_2^* \Delta_1)] \quad (4)$$

with $G = \det\{g_{nn'}\} = g_1 g_2 - g_3^2$. The above expression has to be modified for $G = 0$. In this case the two equations (2) are linearly dependent. As a result, the ratio of the two gaps is the same for all temperatures and magnetic fields $\Delta_2(x)/\Delta_1(x) = g_3/g_1$, while the constant term reduces to $E_{\text{const}} = \int dx |\Delta_1|^2/g_1$.

The standard Gorkov's technique can then be applied to derive the Green's functions and energy spectra in uniform and nonuniform states with and without impurities. In a clean superconductor in zero magnetic field the two superconducting gaps are related via the self-consistent gap equations

$$\Delta_n = \sum_{n'} \lambda_{nn'} \Delta_{n'} \int_0^{\omega_D} \frac{d\varepsilon}{\sqrt{\varepsilon^2 + \Delta_{n'}^2}} \tanh \frac{\sqrt{\varepsilon^2 + \Delta_{n'}^2}}{2T} \quad (5)$$

with dimensionless coupling constants $\lambda_{nn'} = g_{nn'} N_{n'}$, N_n being the density of states at the Fermi level for each band. The transition temperature is given by $T_c = (2\omega_D e^C/\pi) e^{-1/\lambda}$, where ω_D is the Debay frequency, C is the Euler constant and λ is the largest eigenvalue of the matrix $\lambda_{nn'}$:

$$\lambda = (\lambda_{11} + \lambda_{22})/2 + \sqrt{(\lambda_{11} - \lambda_{22})^2/4 + \lambda_{12} \lambda_{21}}. \quad (6)$$

Since $\lambda > \lambda_{11}$, the interband scattering always increases the superconducting transition temperature compared to an instability in a single-band case. The ratio of the two gaps at $T = T_c$ is $\Delta_2/\Delta_1 = \lambda_{21}/(\lambda - \lambda_{22})$. At zero temperature the gap equations (5) are reduced to

$$\Delta_n = \sum_{n'} \lambda_{nn'} \Delta_{n'} \ln \frac{2\omega_D}{\Delta_{n'}}. \quad (7)$$

By substituting $\Delta_n = 2\omega_D r_n e^{-1/\lambda}$ the above equation is transformed to

$$r_n = \sum_{n'} \lambda_{nn'} r_{n'} \left(\frac{1}{\lambda} - \ln r_{n'} \right). \quad (8)$$

For $1/\lambda \gg \ln r_n$, one can neglect logarithms on the right hand side and obtain for the ratio of the two gaps the same equation as at $T = T_c$ implying that Δ_2/Δ_1 is temperature independent.³⁰ This approximation is valid only for $r_n \simeq 1$, *i.e.*, if all the coupling constants $\lambda_{nn'}$ have the same order of magnitude. (For $g_3^2 = g_1 g_2$ the above property is an exact one: the gap ratio does not change neither with temperature nor in magnetic field.) However, for $g_3 \ll g_2 < g_1$, the passive gap Δ_2 is significantly smaller than the active gap Δ_1 and $r_2 \ll 1$ so that the corresponding logarithm cannot be neglected. It follows from Eq. (8) that the ratio Δ_2/Δ_1 increases between $T = T_c$ and $T = 0$ for small g_3 . Such variations become more pronounced in superconductors with larger values of λ , which are away from the extreme weak-coupling limit $\lambda \ll 1$. Ab-initio calculations indicate that MgB₂ has an intermediate strength of the electron-phonon coupling with $\lambda_{12(21)} \ll \lambda_{11} \lesssim 1$, making this superconductor an ideal system to observe effects related to variations of the ratio of two gaps.

The jump in the specific heat at the superconducting transition can be expressed analytically as^{12,30,31}

$$\frac{\Delta C}{C} = \frac{12}{7\zeta(3)} \frac{(N_1 \Delta_1^2 + N_2 \Delta_2^2)^2}{(N_1 + N_2)(N_1 \Delta_1^4 + N_2 \Delta_2^4)}, \quad (9)$$

where the limit $T \rightarrow T_c$ has to be taken for the ratio of the two gaps. The specific heat jump is always smaller than the single-band BCS result $\Delta C/C = 12/7\zeta(3) \approx 1.43$, unless $\Delta_1 = \Delta_2$.

B. Fit to experimental data

One of the striking experimental evidences of the double-gap behavior in MgB₂ is an unusual temperature dependence of the specific heat with a shoulder-type anomaly around $0.25T_c$.^{7,8,9,10} We use here the multi-band BCS theory to fit the experimental data for $C(T)$. The Fermi surface in MgB₂ consists of four sheets: two nearly cylindrical hole sheets arising from quasi two-dimensional $p_{x,y}$ boron bands and two sheets from three-dimensional p_z bonding and antibonding bands.^{13,32} The electronic structure of MgB₂ is now well understood from a number of density-functional studies,^{13,14,15,16,17,18,19} which generally agree with each other, though differ in certain details. Specifically, we choose as a reference the work of Kong *et al.*,¹⁶ where the tight-binding fits for all Fermi surface sheets in MgB₂ are provided. Using these fits we have calculated various Fermi surface averages for each band. The density of states at the Fermi level is $N(0) = 0.41$ states/eV/cell/spin, which includes $N_\sigma(0) = 0.16 = 0.049 + 0.111$ states/eV/cell/spin in light and heavy σ -bands and $N_\pi(0) = 0.25 = 0.124 + 0.126$ states/eV/cell/spin in the two π -bands. Note, that the obtained $N_\pi(0)$ is somewhat larger than the number 0.205 cited by Kong *et al.*,¹⁶ while the results for the σ -bands agree. Because of a strong mismatch in the electron-phonon coupling between two group of

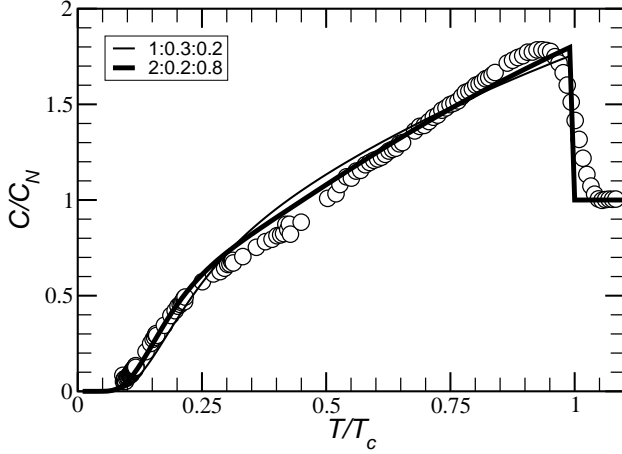


FIG. 1: Theoretical dependence of the specific heat in the two-band BCS model. Numbers for each curve indicate values of g_1 , g_2 , and g_3 ($N_1 = 0.4$, $N_2 = 0.6$). Open circles are the experimental data.^{7,10}

bands,^{15,16,17,18} the two σ -bands can be represented as a single active band, which has $N_1 = 0.4N(0)$ of the total density of states and drives superconducting instability, whereas a combined π -band contributes $N_2 = 0.6N(0)$ to the total density of states and plays a passive role in the superconducting instability. The above numbers are consistent with $N_1 = 0.45N(0)$ and $N_1 = 0.42N(0)$ for the partial density of states of the electrons in the σ -bands obtained in the other studies.^{14,17}

The gap equations (5) have been solved self-consistently for $N_2/N_1 = 1.5$ and various values of coupling constants. The specific heat is calculated from

$$C(T) = \sum_{nk} E_{nk} \frac{dn_F(E_{nk})}{dT}, \quad (10)$$

where $E_{nk} = \sqrt{\varepsilon_k + \Delta_n^2}$ is a quasiparticle energy for each band and $n_F(\varepsilon)$ is the Fermi distribution. Figure 1 shows two theoretical fits to the experimental data of Geneva group^{7,10} using a weak $g_1 N_1 = 0.4$ and a moderate $g_1 N_1 = 0.8$ strength of the coupling constant in the active band. Constants g_2 and g_3 have been varied to get the best fits. In the first case the gap ratio changes in the range $\Delta_1/\Delta_2 = 3\text{--}2.5$ between $T = T_c$ and $T = 0$, while in the second case $\Delta_1/\Delta_2 \simeq 2.7$. Both theoretical curves reproduce quite well the qualitative behavior of $C(T)$. Somewhat better fits can be obtained by increasing the partial density of states in the σ -band. Quantitative discrepancies between various theoretical fits and the experimental data are, however, less significant than differences between different samples.¹⁰ We, therefore, conclude that though the specific heat data clearly agree with the two-gap superconducting model in the regime of weak interband interaction, a unique identification of coupling constants is not possible from available data.

III. THE GINZBURG-LANDAU FUNCTIONAL

We use the microscopic theory formulated in the previous section to derive the Ginzburg-Landau functional of a two-gap superconductor. In the vicinity of T_c the anomalous terms in the mean-field Hamiltonian (3) are treated as a perturbation V_a . Then, the thermodynamic potential of the superconducting state is expressed as

$$\Omega_s = E_{\text{const}} - \frac{1}{\beta} \ln \left\langle T_\tau \exp \left[- \int_0^\beta V_a(\tau) d\tau \right] \right\rangle, \quad (11)$$

where $\beta = 1/T$. Expansion of Eq. (11) in powers of V_a yields the Ginzburg-Landau functional. Since the normal-state Green's functions are diagonal in the band index, the Wick's decoupling of V_a in Ω_s does not produce any mixing terms between the gaps. As a result, the weak-coupling Ginzburg-Landau functional has a single Josephson-type interaction term:

$$\begin{aligned} F_{GL} = & \int dx \left[\alpha_1 |\Delta_1|^2 + \alpha_2 |\Delta_2|^2 - \gamma (\Delta_1^* \Delta_2 + \Delta_2^* \Delta_1) \right. \\ & \left. + \frac{1}{2} \beta_1 |\Delta_1|^4 + \frac{1}{2} \beta_2 |\Delta_2|^4 + K_{1i} |\nabla_i \Delta_1|^2 + K_{2i} |\nabla_i \Delta_2|^2 \right], \\ \nabla_i = & \partial_i + i \frac{2\pi}{\Phi_0} A_i, \quad \alpha_{1,2} = \frac{g_{2,1}}{G} - N_{1,2} \ln \frac{2\omega D e^C}{\pi T}, \quad (12) \\ \beta_n = & \frac{7\zeta(3)N_n}{16\pi^2 T_c^2}, \quad \gamma = \frac{g_3}{G}, \quad K_{ni} = \frac{7\zeta(3)N_n}{16\pi^2 T_c^2} \langle v_{Fn}^2 \rangle, \end{aligned}$$

Φ_0 being the flux quantum. For $\gamma > 0$, the interaction term favors the same phase for the two gaps. For $\gamma < 0$, if, *e.g.*, the Coulomb interactions dominate the interband scattering of the Cooper pairs and $g_3 < 0$, the smaller gap acquires a π -shift relative to the larger gap.^{33,34}

The gradient term coefficients depend in a standard way on the averages of Fermi velocities \mathbf{v}_{Fn} over various sheets of the Fermi surface. Numerical integration of the tight-binding fits¹⁶ yields the following results: for the σ -band $\langle v_{Fx}^2 \rangle = 2.13$ (3.55, 1.51) and $\langle v_{Fz}^2 \rangle = 0.05$ (0.05, 0.05); for the π -band $\langle v_{Fx}^2 \rangle = 1.51$ (1.47, 1.55) and $\langle v_{Fz}^2 \rangle = 2.96$ (2.81, 3.10) in units of $10^{15} \text{ cm}^2/\text{s}^2$, numbers in parentheses correspond to each of the constituent bands. The effective masses of the quasi two-dimensional σ -band exhibit a factor of 40 anisotropy between in-plane and out of plane directions. In contrast, the three-dimensional π -band has a somewhat smaller mass along the c -axis. Using $N_2/N_1 = 1.5$ we find that the in-plane gradient constants for the two bands are practically the same $K_{2\perp}/K_{1\perp} \approx 1.06$, while the c -axis constants differ by almost two orders of magnitude $K_{2z}/K_{1z} \approx 90$.

A very simple form of the two-gap weak-coupling Ginzburg-Landau functional is somewhat unexpected. On general symmetry grounds, there are possible various types of interaction in quartic and gradient terms between two superconducting condensates of the same symmetry, which have been considered in the literature.^{35,36,37} The above form of the Ginzburg-Landau functional is, nevertheless, a straightforward

extension of the well-known result for unconventional superconductors. For example, the quartic term for a momentum-dependent gap is $|\Delta(\mathbf{k})|^4$ in the weak-coupling approximation.^{38,39} In the two-band model $\Delta(\mathbf{k})$ assumes a step-like dependence between different pieces of the Fermi surface, which immediately leads to the expression (12).

The Ginzburg-Landau equations for the two-gap superconductor, which are identical to those obtained from Eq. (12), have been first derived by an expansion of the gap equations in powers of Δ .³⁰ Recently, a similar calculation has been done for a dirty superconductor, with only *intraband* impurity scattering and the corresponding form of the Ginzburg-Landau functional has been guessed, though with incorrect sign of the coupling term.²⁶ Here, we have directly derived the free energy of the two-gap superconductor. The derivation can be straightforwardly generalized to obtain, e.g. higher-order gradient terms, which are needed to find an orientation of the vortex lattice relative to crystal axis (see below). We also note that strong-coupling effects, e.g., dependence of the pairing interactions on the gap amplitudes, will produce other, generally weaker, mixing terms of the fourth order in Δ . The *interband* scattering by impurities can generate a mixing gradient term as well.

Finally, for $G = (g_1 g_2 - g_3^2) < 0$ a number of spurious features appears in the theory: the matrix $\lambda_{nn'}$ and the quadratic form (4) acquire negative eigenvalues, while a formal minimization of the Ginzburg-Landau functional (12) leads to an unphysical solution at high temperatures. Sign of Δ_2/Δ_1 for such a solution is opposite to the sign of g_3 . The origin of this ill-behavior lies in the approximation of positive integrals on the right-hand side of Eq. (5) by logarithms, which can become negative. Therefore, negative eigenvalues of $\lambda_{nn'}$ and E_{const} yield no physical solution similar to the case when the BCS theory is applied to the Fermi gas with repulsion. The consequence for the Ginzburg-Landau theory (12) is that one should keep the correct sign of Δ_2/Δ_1 and use the Ginzburg-Landau equations, *i.e.*, look for a saddle-point solution rather than seeking for an absolute minimum.

IV. THE TWO-GAP GINZBURG-LANDAU THEORY

In order to discuss various properties of a two-gap superconductor in the framework of the Ginzburg-Landau theory we write $\alpha_1 = -a_1 t$ with $a_1 = N_1$, $t = \ln(T_1/T) \approx (1 - T/T_1)$ and $T_1 = (2\omega_D e^C/\pi)e^{-g_2/GN_1}$ for the first active band and $\alpha_2 = \alpha_{20} - a_2 t$ with $a_2 = N_2$, $\alpha_{20} = (\lambda_{11} - \lambda_{22})/GN_1$ for the passive band.

A. Zero magnetic field

For completeness, we briefly mention here the behavior in zero magnetic field. The transition temperature

is found from diagonalization of the quadratic form in Eq. (12):

$$t_c = \frac{\alpha_{20}}{2a_2} - \sqrt{\frac{\alpha_{20}^2}{4a_2^2} + \frac{\gamma^2}{a_1 a_2}}. \quad (13)$$

For small γ , one finds $t_c \approx -\gamma^2/(a_1 \alpha_{20})$. Negative sign of t_c means that the superconducting transition takes place above T_1 , which is an intrinsic temperature of superconducting instability in the first band. The ratio of the two gaps $\rho = \Delta_2/\Delta_1 = \gamma/(\alpha_{20} - a_2 t_c)$. Below the transition temperature, the gap ratio ρ obeys

$$\alpha_2 \rho - \gamma + \frac{\beta_2}{\beta_1} \rho^3 (a_1 t + \gamma \rho) = 0. \quad (14)$$

For small γ , one can approximate $\rho \approx \gamma/\alpha_2$ and due to a decrease of α_2 with temperature, small to large gap ratio ρ increases away from t_c .

B. The upper critical field

1. Magnetic field parallel to the *c*-axis

Due to the rotational symmetry about the *c*-axis, the gradient terms in the *a-b* plane are isotropic and can be described by two constants $K_{n\perp} \equiv K_n$. The linearized Ginzburg-Landau equations describe a system of two coupled oscillators and have a solution in the form $\Delta_1 = c_0 f_0(x)$ and $\Delta_2 = d_0 f_0(x)$, where $f_0(x)$ is a state on the zeroth Landau level. The upper critical field is given by $H_{c2} = h_{c2} \Phi_0 / 2\pi$

$$h_{c2} = \frac{a_1 t}{2K_1} - \frac{\alpha_2}{2K_2} + \sqrt{\left(\frac{a_1 t}{2K_1} + \frac{\alpha_2}{2K_2}\right)^2 + \frac{\gamma^2}{K_1 K_2}} \quad (15)$$

The ratio of the two gaps $\rho = d_0/c_0$ along the upper critical line is

$$\rho = \frac{\gamma}{\alpha_2 + K_2 h_{c2}}. \quad (16)$$

The above expression indicates that an applied magnetic field generally tends to suppress a smaller gap. Whether this effect overcomes an opposite tendency to an increase of Δ_2/Δ_1 due to a decrease of α_2 with temperature depends on the gradient term constants. For example, in the limit $\gamma \ll \alpha_{20}$ we find from (16) $\rho \approx \gamma/[\alpha_{20} - (a_2 - a_1 K_2/K_1)t]$. If K_2 is significantly larger than K_1 , while $a_2 \simeq a_1$, the smaller gap is quickly suppressed along the upper critical field line. However, for MgB₂ one finds $K_2/K_1 \approx 1$ for in-plane gradient terms. Therefore, the ratio Δ_2/Δ_1 continues to grow along $H_{c2}(T)$, though slower than in zero field.

2. Transverse magnetic field

We assume that $\mathbf{H} \parallel \hat{\mathbf{y}}$ and consider a homogeneous superconducting state along the field direction. The gradient terms in two transverse directions $\hat{\mathbf{x}}$ and $\hat{\mathbf{z}}$ have

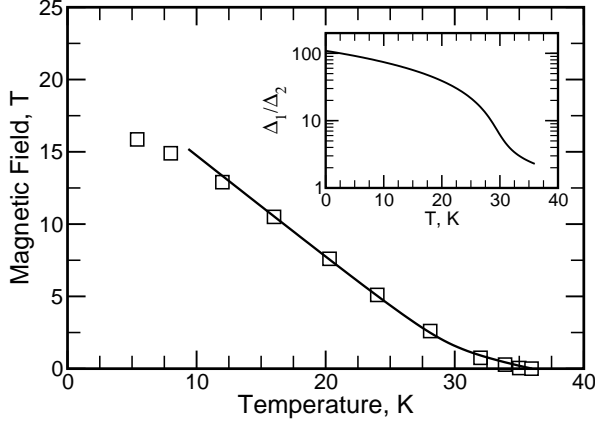


FIG. 2: Temperature dependence of the upper critical field in MgB₂ for magnetic field in the basal plane. Solid line: the two-gap Ginzburg-Landau theory with parameters given in the text, squares: experimental data by Lyard *et al.*⁴⁰ The inset shows variation of the gap ratio along the $H_{c2}(T)$ line for the same set of parameters.

different stiffness constants K_n and K_{nz} , respectively. In a single band case, rescaling $x \rightarrow x(K_x/K_z)^{1/4}$ and $z \rightarrow z(K_z/K_x)^{1/4}$ allows to reduce an anisotropic problem to the isotropic one in rescaled coordinates. A multi-gap superconductor has several different ratios K_n/K_{nz} and the above rescaling procedure does not work. In other words, coupled harmonic oscillators described by the linearized Ginzburg-Landau equations have different resonance frequencies. To solve this problem we follow a variational approach, which is known to give a good accuracy in similar cases. The vector potential is chosen in the Landau gauge $\mathbf{A} = (Hz, 0, 0)$ and we look for a solution in the form

$$\begin{pmatrix} \Delta_1 \\ \Delta_2 \end{pmatrix} = \left(\frac{\lambda}{\pi} \right)^{1/4} e^{-\lambda z^2/2} \begin{pmatrix} c \\ d \end{pmatrix}, \quad (17)$$

where λ , c , and d are variational parameters. After spatial integration and substitution $\lambda = h/\mu$, $h = 2\pi H/\Phi_0$, the quadratic terms in the Ginzburg-Landau functional become

$$\begin{aligned} F_2 = & (-a_1 t + h \tilde{K}_1) |c|^2 + (\alpha_2 + h \tilde{K}_2) |d|^2 \\ & - \gamma (c^* d + d^* c), \quad \tilde{K}_n = \frac{1}{2} (K_n \mu + K_{nz} / \mu) \end{aligned} \quad (18)$$

The determinant of the quadratic form vanishes at the transition into superconducting state. Transition field is given by the same expression as in the isotropic case (15), where K_n have to be replaced with \tilde{K}_n . The upper critical field is, then, obtained from maximizing the corresponding expression with respect to the variational parameter μ . In general, maximization procedure has to be done numerically. Analytic expressions are possible in two temperature regimes. At low temperatures $t \gg |t_c|$, the upper critical field is entirely determined by the ac-

tive band and

$$h_{c2} = \frac{a_1 t}{\sqrt{K_1 K_{1z}}}. \quad (19)$$

In the vicinity of T_c , an external magnetic field has a small effect on the gap ratio $\rho = d/c \approx \gamma/\alpha_{20}$ and an effective single-gap Ginzburg-Landau theory can be applied. The upper critical field is given by a combination of the gradient constants K_{ni} weighted according to the gap amplitudes:

$$h_{c2} = \frac{a_1 (t - t_c)}{\sqrt{(K_1 + \rho^2 K_2)(K_{1z} + \rho^2 K_{2z})}}. \quad (20)$$

Since, in MgB₂ one has $K_{1z} \simeq 0.01 K_{2z}$ and $\rho^2 \simeq 0.1$, the slope of the upper critical field near T_c is determined by an effective gradient constant $K_z^{\text{eff}} \approx \rho^2 K_{2z} > K_{1z}$ (while $(K_1 + \rho^2 K_2) \approx K_1$). Thus, the upper critical field line $H_{c2}(T)$ shows a marked upturn curvature between the two regimes (20) and (19). Such a temperature behavior has been recently addressed in a number of theoretical works based on various forms of the two-band BCS theory.^{24,25,26,27} We suggest here a simpler description of the above effect within the two-gap Ginzburg-Landau theory.

Finally, we compare the Ginzburg-Landau theory with the experimental data on the temperature dependence of the upper critical field for magnetic field parallel to the basal plane.⁴⁰ We choose ratios of the gradient term constants and the densities of states in accordance with the band structure calculations¹⁶ and change parameters γ and α_{20} , which are known less accurately, to fit the experimental data. The best fit shown in Fig. 2 is obtained for $\alpha_{20}/a_1 = 0.65$ and $\gamma/a_1 = 0.4$. The prominent upward curvature of $H_{c2}(T)$ takes place between $t_c = -0.18$ ($T_c = 36$ K) and $t \simeq 0.2$ ($T = 26$ K), i.e. well within the range of validity of the Ginzburg-Landau theory. The above values of α_{20} and γ can be related to g_2/g_1 and g_3/g_1 and they appear to be closer to the second choice of g_n used for Fig. (1). The ratio of the two gaps, as it changes along the $H_{c2}(T)$ line, is shown on the inset in Fig. 2. It varies from $\Delta_1/\Delta_2 \approx 2.3$ near $T_c = 36$ K to $\Delta_1/\Delta_2 \approx 45$ at $T = 18$ K, where the Ginzburg-Landau theory breaks down. Due to a large difference in the c -axis coherence lengths between the two bands, the smaller gap is quickly suppressed by transverse magnetic field. Also, the strong upward curvature of $H_{c2}(T)$ leads to temperature variations of the anisotropy ratio $\gamma_{\text{an}} = H_{c2}^{\perp}(T)/H_{c2}^c(T)$, which changes from $\gamma_{\text{an}} = 1.7$ near T_c to $\gamma_{\text{an}} = 4.3$ at $T = 18$ K. These values are again consistent with experimental observations,⁴¹ as well as with theoretical studies.^{24,25,26}

C. Structure of a single vortex

The structure of an isolated superconducting vortex parallel to the c -axis has been studied in MgB₂ by the

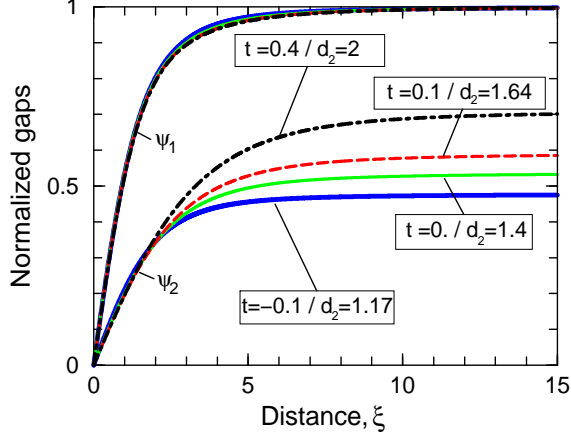


FIG. 3: Spatial dependencies of the gaps for various temperatures with $t = \ln T_1/T \approx 1 - T/T_1$ and $K_2/K_1 = 9$.

scanning tunneling microscopy.⁴² Tunneling along the c -axis used in the experiment probes predominantly the three-dimensional π -band and the obtained spectra provide information about a small passive gap. A large vortex core size of about 5 coherence lengths $\xi_c = \sqrt{\Phi_0/2\pi H_{c2}^c}$ was reported and attributed to a fast suppression of a passive gap by magnetic field, whereas the c -axis upper critical field is controlled by a large gap in the σ -band.⁴² The experimental observations were confirmed within the two-band model using the Bogoliubov-de Gennes²³ and the Usadel equations.²⁸ We have, however, seen in the previous Subsection that a π -gap in MgB₂ is not suppressed near $H_{c2}(T)$ for fields applied along the c -axis. To resolve this discrepancy we present here a systematic study of the vortex core in a two-gap superconductor in the framework of the Ginzburg-Landau theory.

We investigate the structure of a single-quantum vortex oriented parallel to the hexagonal c -axis. The two gaps are parametrized as $\Delta_n(\mathbf{r}) = \psi_n(r)e^{-i\theta}$, where θ is an azimuthal angle and r is a distance from the vortex axis. Since the Ginzburg-Landau parameter for MgB₂ is quite large,² $\kappa \simeq 25$, magnetic field can be neglected inside vortex core leading to the following system of the Ginzburg-Landau equations

$$\alpha_n \psi_n - \gamma \psi_n' + \beta_n \psi_n^3 - K_n(\psi_n'' + \psi_n'/r - Q^2 \psi_n) = 0 \quad (21)$$

for $n = 1, 2$ ($n' = 2, 1$) and $Q \approx 1/r$. Away from the center of a vortex, the two gaps approach their asymptotic amplitudes ψ_{0n}

$$\psi_{01} = \sqrt{\frac{a_1 t + \gamma \rho}{\beta_1}}, \quad \psi_{02} = \sqrt{\frac{\gamma/\rho - \alpha_2}{\beta_2}} \quad (22)$$

with ρ obeying Eq. (14). All distances are measured in units of a temperature-dependent coherence length derived from the upper critical field Eq. (15). In order to

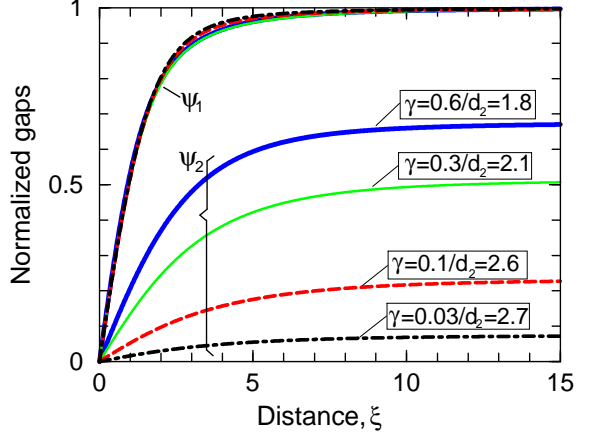


FIG. 4: Spatial dependencies of the gaps for various values of γ (given in units of a_1) for $t = 0.3$ and $K_2/K_1 = 9$.

solve Eq. (21) numerically, a relaxation method has been used⁴³ on a linear array of 4000 points uniformly set on a length of 80ξ from the vortex center. An achieved accuracy is of the order of 10^{-6} .

The obtained results are shown in Figures 3–5, where amplitudes $\psi_n(r)$ are normalized to the asymptotic value of the large gap ψ_{01} . To quantify the size of the vortex core for each component we determine the distance d_n , where $\psi_n(r)$ reaches a half of its maximum value ψ_{0n} . In the case of a single-gap superconductor such a distance is given within a few percent by the coherence length. In a two-gap superconductor the characteristic length scale for the large gap d_1 remains close to ξ , while d_2 can substantially vary. Size of the vortex core is given by $d_v = \max(2d_1, 2d_2)$.

Results for temperature dependence of the vortex core are presented in Fig. 3. The parameters α_{20} and γ are taken the same as in the study of the upper critical field, while we choose $K_2/K_1 = 9$ in order to amplify effect for the small gap. As was discussed above, the equilibrium ratio of the two gaps ψ_{02}/ψ_{01} grows with decreasing temperature (increasing t). Simultaneously, the small gap becomes less constrained with its interaction to the large gap and the half-amplitude distance d_2 shows a noticeable growth. For $K_2 \approx K_1$ such a less constrained behavior of $\psi_2(r)$ at low temperatures does not lead to an increase of the core size because both gaps have similar intrinsic coherence lengths.

This trend becomes more obvious if the coupling constant γ is changed for fixed values of all other parameters, see Fig. 4. For vanishing γ , the distance d_2 approaches asymptotically an intrinsic coherence length in the passive band. This length scale depends on K_2 ($d_2/d_1|_{\gamma=0} \simeq \sqrt{K_2/K_1} = 3$), but is not directly related to an equilibrium value of the small gap: the small gap is reduced by a factor of 7 between $\gamma = 0.6$ and $\gamma = 0.03$, while the core size increases by 50% only. Therefore, the single-band BCS estimate $\xi_2 = v_F/(\pi\Delta_2)$ for the char-

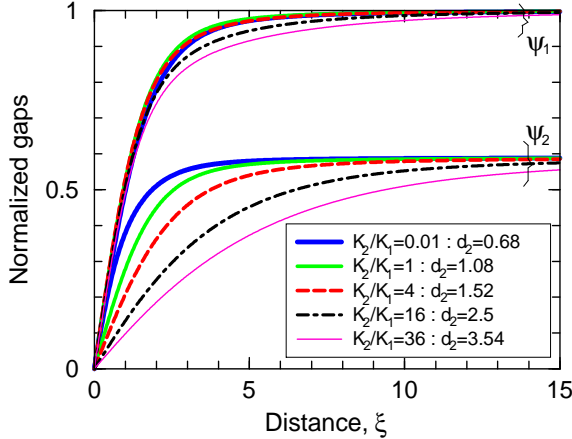


FIG. 5: Spatial dependencies of the gaps for various values of K_2/K_1 for $t = 0.3$.

acteristic length scale of the small gap sometimes used for interpretation of experimental data⁴² is not, in fact, applicable for a multi-gap superconductor.

Finally, Fig. 5 presents evolution of the vortex core with varying ratio K_2/K_1 , where again $\alpha_{20}/a_1 = 0.65$ and $\gamma/a_1 = 0.4$. The apparent size of the vortex core $d_v \simeq 2d_2$ becomes about 5–6 coherence lengths for K_2 exceeding K_1 by an order of magnitude. For $K_2/K_1 \simeq 1$, which follows from the band structure calculations, the vortex core size does not change significantly compared to the standard single-gap case. These results generally agree with the previous study,²⁸ though we conclude that unrealistically large values of K_2/K_1 are required to explain the experiment.⁴² Different strength of impurity scattering in the two bands cannot explain this discrepancy either. It is argued that the π -band is in the dirty limit.²² The coefficient K_2 in Eq. (12) is accordingly replaced by a *smaller* diffusion constant. The numerical results (Fig. 5) as well as qualitative consideration show that in such a case the core size for $\psi_2(r)$ can only decrease. Note, that the spatial ansatz $\psi(r) \sim \tanh(r/a)$ with $a = \xi$ used to fit the experimental data⁴² should be applied with $a = 1.8\xi$ even for a single-gap superconductor in the large κ limit.⁴⁴

V. ORIENTATION OF VORTEX LATTICE

Recent neutron scattering measurements²⁹ in MgB₂ for fields along the hexagonal c -axis have discovered a new interesting phase transition in the mixed state of this superconductor: a triangular vortex lattice rotates by 30° such that below the first transition field (0.5 T at $T = 2$ K) a nearest-neighbor direction is aligned perpendicular to the crystal a -axis, whereas above the second transition field (0.9 T) the shortest intervortex spacing is parallel to the a -axis.²⁹ We show in this section that such

a peculiar behavior is determined by the two-gap nature of superconductivity in MgB₂.

A. Single-gap superconductor

An orientation of the flux line lattice in tetragonal and cubic superconductors has been theoretically studied by Takanaka.⁴⁵ Recently, similar crystal field effects were found to be responsible for the formation of the square vortex lattices in the borocarbides.^{46,47} The case of a single-gap hexagonal superconductor is treated by a straightforward generalization of the previous works. Symmetry arguments suggest that coupling between the superconducting order parameter and a hexagonal crystal lattice appears at the sixth-order gradient terms in the Ginzburg-Landau functional. For simplicity, we assume that gap anisotropy is negligible. Then, the six-order gradient terms derived from the BCS theory are

$$F_6 = \frac{\zeta(7)N_0}{32\pi^6 T_c^6} \left(1 - \frac{1}{2^7}\right) \langle v_{Fi} v_{Fj} v_{Fk} v_{Fl} v_{Fm} v_{Fn} \rangle \times (\nabla_i \nabla_j \nabla_k \Delta^*) (\nabla_l \nabla_m \nabla_n \Delta) . \quad (23)$$

The above terms can be split into isotropic part and anisotropic contribution, the latter being

$$\begin{aligned} F_6^{\text{an}} &= -\frac{\zeta(7)N_0}{64\pi^6 T_c^6} \left(1 - \frac{1}{2^7}\right) (\langle v_{Fx}^6 \rangle - \langle v_{Fy}^6 \rangle) \\ &\times \Delta^* \left[\nabla_x^6 - 15\nabla_x^4 \nabla_y^2 + 15\nabla_x^2 \nabla_y^4 - \nabla_y^6 \right] \Delta \quad (24) \\ &= -\frac{1}{2} K_6 \Delta^* \left[(\nabla_x + i\nabla_y)^6 + (\nabla_x - i\nabla_y)^6 \right] \Delta . \end{aligned}$$

In this expression $\hat{\mathbf{x}}$ is fixed to the a -axis in the basal plane. (An alternative choice is the b -axis.) If $\hat{\mathbf{x}}$ and $\hat{\mathbf{y}}$ are simultaneously rotated by angle φ about the c -axis, $(\nabla_x \pm i\nabla_y)^6$ acquires an extra factor $e^{\pm 6i\varphi}$. In the following we always make such a rotation in order to have $\hat{\mathbf{x}}$ pointing between nearest-neighbor vortices. Periodic Abrikosov solutions with chains of vortices parallel to the x -axis are most easily written in the Landau gauge $\mathbf{A} = (-Hy, 0, 0)$.⁴⁸

The higher order gradient terms Eq. (24) give a small factor $H^2 \sim (1 - T/T_c)^2$ and can be treated as a perturbation in the Ginzburg-Landau regime. The Landau levels expansion yields $\Delta(x) = c_0 f_0(x) + c_6 f_6(x) + \dots$, where the coefficient for the admixed sixth Landau level is $c_6/c_0 \approx -(\sqrt{6}/3)h^2 e^{6i\varphi} K_6/K$. When substituted into the quartic Ginzburg-Landau term, this expression produces the following angular dependent part of the free energy:

$$\delta F(\varphi) = -\frac{2\sqrt{6}K_6}{3K} h_{c2}^2 \beta |c_0|^4 \langle |f_0|^2 f_0^* f_6 \rangle \cos(6\varphi) , \quad (25)$$

with $|c_0|^2 = K(h_{c2} - h) \langle |f_0|^2 \rangle / (\beta \langle |f_0|^4 \rangle)$. Spatial averaging of the combination of the Landau levels is done in

a standard way

$$\begin{aligned} \frac{\langle |f_0|^2 f_0^* f_6 \rangle}{\langle |f_0|^2 \rangle^2} &= \frac{\sqrt{\sigma}}{12\sqrt{5}} \sum_{n,m} \cos(2\pi\rho nm) e^{-\pi\sigma(n^2+m^2)} \\ &\times \left[\pi^3 \sigma^3 (n-m)^6 - \frac{15}{2} \pi^2 \sigma^2 (n-m)^4 \right. \\ &\left. + \frac{45}{4} \pi \sigma (n-m)^2 - \frac{15}{8} \right], \end{aligned} \quad (26)$$

where summation goes over all integer n and m and parameters ρ and σ describe an arbitrary vortex lattice.⁴⁸ For a hexagonal lattice ($\rho = 1/2$, $\sigma = \sqrt{3}/2$), the numerical value of the lattice factor is $\langle |f_0|^2 f_0^* f_6 \rangle / \langle |f_0|^4 \rangle = -0.279$. Hence, $\delta F(\varphi) \simeq +K_6 \cos(6\varphi)$ and for $\langle v_{Fx}^6 \rangle > \langle v_{Fy}^6 \rangle$ ($K_6 > 0$) the equilibrium angle is $\varphi = \pi/2$ ($\pi/6$), which means that the shortest spacing between vortices in a triangular lattice is oriented perpendicular to the a -axis, while for the other sign of anisotropy the shortest side of a vortex triangle is along the a -axis. Thus, the Fermi surface anisotropy fixes uniquely the orientation of the flux line lattice near the upper critical field.

B. Two-gap superconductor

In a multiband superconductor effect of crystal anisotropy may vary from one sheet of the Fermi surface to another. We apply again the tight-binding representation¹⁶ to obtain a quantitative insight about such effects in MgB₂. Explicit expressions for dispersions of the two hole σ -bands are presented in the Appendix. Hexagonal anisotropy in the narrow σ -cylinders is enhanced by a nonanalytic form of the hole dispersions. Combined anisotropy of the σ -band is $\langle v_{Fx}^6 \rangle = 4.608$, $\langle v_{Fy}^6 \rangle = 4.601$, while for the π -band $\langle v_{Fx}^6 \rangle = 1.514$, $\langle v_{Fy}^6 \rangle = 1.776$ in units of 10^{46} (cm/s)⁶. According to the choice of the coordinate system,¹⁶ the \hat{x} -axis is parallel to the b -direction and the \hat{y} -axis is parallel to the a -direction in the boron plane. The above values might be not very accurate due to uncertainty of the LDA results, however, they suggest two special qualitative features for MgB₂. First, relative hexagonal anisotropy of the Fermi velocity $v_{Fn}(\varphi)$ differs by almost two orders of magnitude between the two sets of bands. Second, corresponding hexagonal terms have different signs in the two bands. In Appendix, we have shown that the sign difference is a robust feature of the tight-binding approximation and cannot be changed by a small change of the tight-binding parameters.

We investigate equilibrium orientation of the vortex lattice in MgB₂ within the two-gap Ginzburg-Landau theory. Anisotropic sixth-order gradient terms of the type (24) have to be added to the functional (12) separately for each of the two superconducting order parameters. As was discussed in the previous paragraph the anisotropy constants have different signs $K_{61} > 0$ and $K_{62} < 0$ and obey $|K_{61}| \ll |K_{62}|$. In the vicinity of the upper critical field the two gaps are expanded as $\Delta_1(x) =$

$c_0 f_0(x) + c_6 f_6(x)$ and $\Delta_2(x) = d_0 f_0(x) + d_6 f_6(x)$. Solution of the linearized Ginzburg-Landau equations yields the following amplitudes for the sixth Landau levels:

$$\begin{aligned} c_6 &= -4\sqrt{6!}h^3 e^{6i\varphi} \frac{K_{61}\tilde{\alpha}_2 c_0 + K_{62}\gamma d_0}{\tilde{\alpha}_1\tilde{\alpha}_2 - \gamma^2}, \\ d_6 &= -4\sqrt{6!}h^3 e^{6i\varphi} \frac{K_{62}\tilde{\alpha}_1 d_0 + K_{61}\gamma c_0}{\tilde{\alpha}_1\tilde{\alpha}_2 - \gamma^2} \end{aligned} \quad (27)$$

with $\tilde{\alpha}_{1,2} = \alpha_{1,2} + 13K_{1,2}h$. Subsequent calculations follow closely the single-gap case from the preceding subsection. The angular dependent part of the free energy is obtained by substituting (27) into the fourth-order terms:

$$\delta F(\varphi) = \left[\beta_1 c_0^3 (c_6 + c_6^*) + \beta_2 d_0^3 (d_6 + d_6^*) \right] \langle |f_0|^2 f_0^* f_6 \rangle. \quad (28)$$

The resulting expression can be greatly simplified if one uses $(\Delta_2/\Delta_1)^2 \simeq 0.1$ as a small parameter. With accuracy $O[(\Delta_2/\Delta_1)^4]$ we can neglect the angular dependent part determined by the small gap. This yields in a close analogy with Eq. (25) the following anisotropy energy for the vortex lattice near H_{c2}

$$\begin{aligned} \delta F(\varphi) &= -\frac{2\sqrt{6!}}{3K_1} h_{c2}^2 \beta_1 |c_0|^4 \langle |f_0|^2 f_0^* f_6 \rangle K_6^{\text{eff}} \cos(6\varphi), \\ K_6^{\text{eff}} &= K_{61} + K_{62} \frac{\gamma^2}{(\alpha_2 + K_2 h)(\alpha_2 + 13K_2 h)}. \end{aligned} \quad (29)$$

Despite the fact that we have omitted terms $\sim d_0^3 d_6$, the Fermi surface anisotropy of the second band still contributes to the effective anisotropy constant K_6^{eff} via linearized Ginzburg-Landau equations. Along the upper critical line this contribution decreases suggesting the following scenario for MgB₂.

In the region near T_c the second band makes the largest contribution to K_6^{eff} : a small factor $\gamma^2/\alpha_2^2 \sim 0.1$ is outweighed by $|K_{61}/K_{62}| < 0.1$. As a result, K_6^{eff} is negative and $\varphi = 0$, which means that the shortest intervortex spacing is parallel to the b -axis. At lower temperatures and higher magnetic fields the second term in K_6^{eff} decreases and the Fermi surface anisotropy of the first band starts to determine the (positive) sign of K_6^{eff} . In this case, $\varphi = \pi/2$ ($\pi/6$) and the side of the vortex triangle is parallel to the a -axis. The very small $|K_{61}/K_{62}| = 1.8 \cdot 10^{-2}$, which follows from the band structure data,¹⁶ is insufficient to have such a reorientation transition in the Ginzburg-Landau region. Absolute values of anisotropy coefficients are, however, quite sensitive to the precise values of the tight-binding parameters and it is reasonable to assume that experimental values of K_{6n} are such that the reorientation transition is allowed.

The derived sequence of the orientations of the flux line lattice in MgB₂ completely agrees with the neutron scattering data,²⁹ though we have used a different scan line in the H - T plane in order to demonstrate the presence of the 30°-orientational transformation, see Fig. 6. Condition $K_6^{\text{eff}} = 0$, or similar one applied to Eq. (28), defines a line $H^*(T)$ in the H - T plane, which has a negative

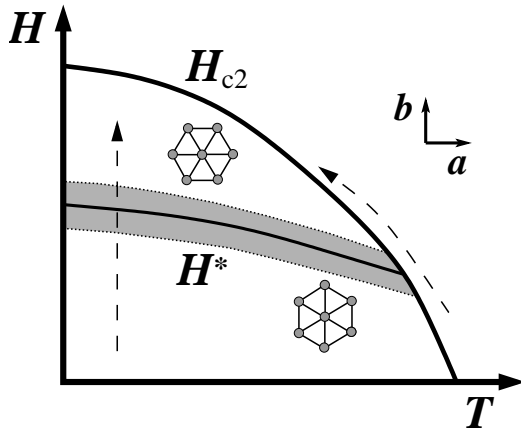


FIG. 6: Phase diagram of MgB_2 for fields parallel to the c -axis. Shaded region corresponds to intermediate orientations of the vortex lattice separated by dotted lines of the second-order transitions. Dashed lines indicate the scans used in the experiment (vertical) and in the presented theory.

slope at the crossing point with $H_{c2}(T)$. The six-fold anisotropy for the vortex lattice vanishes along $H^*(T)$ and all orientations with different angles φ become degenerate in the adopted approximation. The sequence of orientational phase transition in such a case depends on weaker higher-order harmonics. One can generally write

$$\delta F(\varphi) = K_6 \cos(6\varphi) + K_{12} \cos(12\varphi), \quad (30)$$

where the higher-order harmonics comes with a small coefficient $|K_{12}| \ll |K_6|$. Depending on the sign of K_{12} transformation between low-field $\varphi = 0$ and high-field $\varphi = \pi/6$ ($\pi/2$) orientations, when K_6 changes sign, goes either via two second-order transitions ($K_{12} > 0$) or via single first-order transition ($K_{12} < 0$). In the former case the transitions take place at $K_6 = \pm 4K_{12}$, whereas in the latter case the first-order transition is at $K_6 = 0$. These conclusions are easily obtained by comparing the energy of a saddle-point solution $\cos(6\varphi) = -K_6/(4K_{12})$ for Eq. (30), which is $\delta F_{sp} = -K_6^2/(8K_{12})$, to the energies of two extreme orientations.

In order to determine sign of the higher-order harmonics for a two-gap superconductor we expand the fourth-order terms in the Ginzburg-Landau functional (12) to the next order

$$\delta F'(\varphi) = \frac{1}{2} \left[\beta_1 c_0^2 (c_6^2 + c_6^{*2}) + \beta_2 d_0^2 (d_6^2 + d_6^{*2}) \right] \langle f_0^{*2} f_6^2 \rangle. \quad (31)$$

These terms are responsible for a $\cos(12\varphi)$ anisotropy introduced before. Similar angular dependence is also induced by higher-order harmonics of the Fermi velocity $v_F(\varphi)$, though our estimate shows that even for the π -bands corresponding modulations are very small.⁴⁹ Sign of $\cos(12\varphi)$ term in Eq. (31) depends only on a geometric factor, spatial average of the Landau levels wave functions. We find for a perfect triangular lattice

$\langle f_0^{*2} f_6^2 \rangle / \langle |f_0|^2 \rangle^2 = 0.804$. Thus, the twelfth-order harmonics in Eq. (30) has a positive coefficient and transformation between the low-field state with $\varphi = 0$ and the high-field state $\varphi = \pi/6$ goes via a phase with intermediate values of φ separated by two second order transitions.

The anisotropy terms of the type (24) also produce a six-fold modulation of the upper critical field in the basal plane. Sign of the corresponding modulations of $H_{c2}(\varphi)$ should also change at a certain temperature, which is determined by a suppression of the small gap in transverse magnetic field and is not, therefore, related to the intersection point of $H_{c2}(T)$ and $H^*(T)$ lines on the phase diagram for $H \parallel c$, Fig. 6.

VI. CONCLUSIONS

We have derived the Ginzburg-Landau functional of a two-gap superconductor within the weak-coupling BCS theory. The functional contains only a single interaction term between the two superconducting gaps (condensates). This property allows a meaningful analysis of various magnetic properties of a multi-gap superconductor in the framework of the Ginzburg-Landau theory. Apart from confirming the previous results on an unusual temperature dependence of the transverse upper critical field in MgB_2 , we have presented detailed investigation of the vortex core structure and have shown that the orientational phase transitions observed in the flux line lattice in MgB_2 is a manifestation of the multi-band nature of superconductivity in this material. The proposed minimal model for the 30° -rotation of the vortex lattice includes only anisotropy of the Fermi surface. An additional source of six-fold anisotropy for the vortex lattice can arise from angular dependence of the superconducting gap. It was argued that the latter source of (four-fold) anisotropy is essential for physics of the square to distorted triangular lattice transition in the mixed state of borocarbides.⁵⁰ For phonon-mediated superconductivity in MgB_2 , the gap modulations should be quite small, especially for the large gap on the narrow σ -cylinders of the Fermi surface. Experimentally, the role of gap anisotropy can be judged from the position of $H^*(T)$ line in the H - T plane. $H^*(T)$ does not cross $H_{c2}(T)$ line in scenarios with significant gap anisotropy.⁵⁰ A further insight in anisotropic properties of different Fermi surface sheets in MgB_2 can be obtained by studying experimentally and theoretically the hexagonal anisotropy of the upper critical field in the basal plane.

Acknowledgments

The authors would like to acknowledge useful discussions with R. Cubitt, M. R. Eskildsen, V. M. Gvozdikov, A. G. M. Jansen, S. M. Kazakov, K. Machida, I. I. Mazin, and V. P. Mineev. We also thank F. Bouquet and P. Samuely for providing their experimental data.

APPENDIX: ANISOTROPY IN σ -BANDS

We give here expressions for the dispersions and Fermi surface anisotropies in the two σ -bands, which are derived from the tight-binding fits of Kong *et al.*¹⁶ The in-plane $p_{x,y}$ boron orbitals in MgB₂ undergo an sp^2 -hybridization with s -orbitals and form three bonding bands. At $\mathbf{k}_\perp = 0$ these bands are split into a non-degenerate A -symmetric band and doubly-degenerate E -symmetric band, which lies slightly above the Fermi level. Away from the $\mathbf{k}_\perp = 0$ -line the E -band splits into light and heavy hole bands. Their dispersions obtained by expansion of the tight-binding matrix¹⁶ in small k_\perp are

$$\begin{aligned}\varepsilon_l(\mathbf{k}) &= \varepsilon(k_z) - 2t_\perp \left[\frac{1}{8}k_\perp^2 + dk_\perp^4 \frac{2g(\mathbf{k}) + 1 - 1/d}{384(1+d)} \right], \\ \varepsilon_h(\mathbf{k}) &= \varepsilon(k_z) - 2t_\perp \left[\frac{3}{8}dk_\perp^2 - dk_\perp^4 \frac{2g(\mathbf{k}) + 7 + 9d}{384(1+d)} \right],\end{aligned}$$

where $\varepsilon(k_z) = \varepsilon_0 - 2t_z \cos k_z$ and $g(\mathbf{k}) = (k_x^6 - 15k_x^4k_y^2 + 15k_x^2k_y^4 - k_y^6)/k_\perp^6$. The tight-binding parameters presented in Ref. 16 are $\varepsilon_0 = 0.58$ eV, $t_\perp = 5.69$ eV, $t_z = 0.094$ eV, and $d = 0.16$. The six-fold anisotropy is given by unusual nonanalytic terms, which are formally of the fourth order in k . Appearance of such nonanalytic terms is a direct consequence of the degeneracy of the two bands at $k = 0$. For example, a nonanalytic form of $\varepsilon(\mathbf{k})$ is known for four-fold degenerate hole bands of Si and Ge,⁵¹ which have cubic anisotropy already in $O(k^2)$ order. Nonanalyticity of $\varepsilon_{l,h}(\mathbf{k})$ leads to a relative enhancement of the hexagonal anisotropy on two narrow Fermi surface cylinders. This anisotropy has opposite sign in light- and heavy-hole bands. The net anisotropy of the combined σ -band is determined mostly by the light-holes, which have larger in-plane Fermi velocities.

- ¹ J. Nagamatsu, N. Nakagawa, T. Muranaka, Y. Zenitani, and J. Akimitsu, *Nature* **410**, 63 (2001).
- ² see for review P. C. Canfield, S. L. Bud'ko, and D. K. Finnemore, *Physica C* **385**, 1 (2003) and other articles in this issue.
- ³ F. Giubileo, D. Roditchev, W. Sacks, R. Lamy, D. X. Thanh, J. Klein, S. Miraglia, D. Fruchart, J. Marcus, and P. Monod, *Phys. Rev. Lett.* **87**, 177008 (2001).
- ⁴ M. Iavarone, G. Karapetrov, A. E. Koshelev, W. K. Kwok, G. W. Crabtree, D. G. Hinks, W. N. Kang, E.-M. Choi, H. J. Kim, H. J. Kim, and S. I. Lee, *Phys. Rev. Lett.* **89**, 187002 (2002).
- ⁵ P. Szabo, P. Samuely, J. Kacmarcik, T. Klein, J. Marcus, D. Fruchart, S. Miraglia, C. Mercenat, and A. G. M. Jansen, *Phys. Rev. Lett.* **87**, 137005 (2001).
- ⁶ H. Schmidt, J. F. Zasadzinski, K. E. Gray and D. G. Hinks, *Phys. Rev. Lett.* **88**, 127002 (2001).
- ⁷ Y. Wang, T. Plackowski, and A. Junod, *Physica C* **355**, 179 (2001).
- ⁸ F. Bouquet, R. A. Fisher, N. E. Phillips, D. G. Hinks, and J. D. Jorgensen, *Phys. Rev. Lett.* **87**, 47001 (2001).
- ⁹ H. D. Yang, J.-Y. Lin, H. H. Li, F. H. Hsu, C. J. Liu, S.-C. Li, R.-C. Yu, and C.-Q. Jin, *Phys. Rev. Lett.* **87**, 167003 (2001).
- ¹⁰ F. Bouquet, Y. Wang, R. A. Fisher, D. G. Hinks, J. D. Jorgensen, A. Junod and N. E. Phillips, *Europhys. Lett.* **56**, 856 (2001).
- ¹¹ H. Suhl, B. T. Matthias, and L. R. Walker, *Phys. Rev. Lett.* **3**, 552 (1959).
- ¹² V. A. Moskalenko, *Fiz. Met. Metalloved.* **8**, 503 (1959) [Sov. Phys. Met. Matallogr. **8**, 25 (1959)].
- ¹³ J. Kortus, I. I. Mazin, K. D. Belashchenko, V. P. Antropov, and L. L. Boyer, *Phys. Rev. Lett.* **86**, 4656 (2001).
- ¹⁴ K. D. Belashchenko, M. van Schilfgaarde, and V. P. Antropov, *Phys. Rev. B* **64**, 092503 (2001).
- ¹⁵ J. M. An and W. E. Pickett, *Phys. Rev. Lett.* **86**, 4366 (2001).
- ¹⁶ Y. Kong, O. V. Dolgov, O. Jepsen, and O. K. Andersen, *Phys. Rev. B* **64**, 020501 (2001).
- ¹⁷ A. Y. Liu, I. I. Mazin, and J. Kortus, *Phys. Rev. Lett.* **87**, 087005 (2001).
- ¹⁸ H. J. Choi, D. Roudny, H. Sun, M. L. Cohen, and S. G. Louie, *Nature* **418**, 758 (2002).
- ¹⁹ I. I. Mazin and V. P. Antropov, *Physica C* **385**, 49 (2003).
- ²⁰ A. A. Golubov, J. Kortus, O. V. Dolgov, O. Jepsen, Y. Kong, O. K. Andersen, B. J. Gibson, K. Ahn, and R. K. Kremer, *J. Phys.: Condens. Matter* **14**, 1353 (2002).
- ²¹ A. Brinkman, A. A. Golubov, H. Rogalla, O. V. Dolgov, J. Kortus, Y. Kong, O. Jepsen, O. K. Andersen, *Phys. Rev. B* **65**, 180517 (2002).
- ²² I. I. Mazin, O. K. Andersen, O. Jepsen, O. V. Dolgov, J. Kortus, A. A. Golubov, A. B. Kuz'menko, and D. van der Marel, *Phys. Rev. Lett.* **89**, 107002 (2002).
- ²³ A. Nakai, M. Ichioka, and K. Machida, *J. Phys. Soc. Jpn.* **71**, 23 (2002).
- ²⁴ P. Miranovic, K. Machida, and V. G. Kogan, *J. Phys. Soc. Jpn.* **72**, 221 (2003).
- ²⁵ T. Dahm and N. Schopohl, *Phys. Rev. Lett.* **91**, 017001 (2003); T. Dahm, S. Graser, and N. Schopohl, *cond-mat/0304194*.
- ²⁶ A. Gurevich, *Phys. Rev. B* **67**, 184515 (2003).
- ²⁷ A. A. Golubov and A. E. Koshelev, *cond-mat/0303237*.
- ²⁸ A. E. Koshelev and A. A. Golubov, *Phys. Rev. Lett.* **90**, 177002 (2003).
- ²⁹ R. Cubitt, M. R. Eskildsen, C. D. Dewhurst, J. Jun, S. M. Kazakov, and J. Karpinski, *Phys. Rev. Lett.* **91**, 047002 (2003).
- ³⁰ B. T. Geilikman, R. O. Zaitsev, V. Z. Kresin, *Fiz. Tverd. Tela* **9**, 821 (1967) [Sov. Phys. Solid State **9**, 642 (1967)].
- ³¹ T. Mishonov and E. Penev, *Int. J. Mod. Phys. B* **16**, 3573 (2002).
- ³² J. K. Burdett and G. J. Miller, *Chem. Mater.* **2**, 12 (1989); A. I. Ivanovskii and N. I. Medvedeva, *Russ. J. Inorg. Chem.* **45**, 1234 (2000).
- ³³ A. A. Golubov and I. I. Mazin, *Physica C* **243**, 153 (1995).
- ³⁴ M. Imada, *J. Phys. Soc. Jpn.* **70**, 1218 (2001).
- ³⁵ H. Doh, M. Sigrist, B. K. Cho, and S. I. Lee, *Phys. Rev. Lett.* **83**, 5350 (1999).
- ³⁶ J. J. Betouras, V. A. Ivanov, and F. M. Peeters, *Eur. J. Phys.* **31**, 349 (2003).

³⁷ A. Gurevich and V. M. Vinokur, Phys. Rev. Lett. **90**, 047004 (2003).

³⁸ L. P. Gor'kov and T. K. Melik-Barkhudarov, Zh. Eksp. Teor. Fiz. **45**, 1493 (1963) [Sov. Phys. JETP **18**, 1031 (1964)].

³⁹ A. J. Leggett, Rev. Mod. Phys. **47**, 331 (1975).

⁴⁰ L. Lyard, P. Samuely, P. Szabo, T. Klein, C. Marcenat, L. Paulius, K. H. P. Kim, C. U. Jung, H.-S. Lee, B. Kang, S. Choi, S.-I. Lee, J. Marcus, S. Blanchard, A. G. M. Jansen, U. Welp, G. Karapetrov, and W. K. Kwok, Phys. Rev. B **66**, 180502 (2002).

⁴¹ R. Cubitt, S. Levett, S. L. Bud'ko, N. E. Anderson, and P. C. Canfield, Phys. Rev. Lett. **90**, 157002 (2003).

⁴² M. R. Eskildsen, M. Kugler, S. Tanaka, J. Jun, S. M. Kazakov, J. Karpinski, and O. Fischer, Phys. Rev. Lett. **89**, 187003 (2002).

⁴³ *Numerical-recipes in Fortran: the art of scientific computing*, W. H. Press, B. P. Flannery, S. A. Teukolsky, W. T. Vetterling, Cambridge University Press (2002).

⁴⁴ C.-R. Hu, Phys. Rev. B **6**, 1756 (1972).

⁴⁵ K. Takanaka, Prog. Theor. Phys. **46**, 1301 (1971).

⁴⁶ Y. De Wilde, M. Iavarone, U. Welp, V. Metlushko, A. E. Koshelev, I. Aranson, G. W. Crabtree, and P. C. Canfield, Phys. Rev. Lett. **78**, 4273 (1997).

⁴⁷ K. Park and D. A. Huse, Phys. Rev. B **58**, 9427 (1998).

⁴⁸ D. Saint-James, E. J. Thomas, and G. Sarma, *Type II Superconductivity* (Pergamon Press, Oxford, 1969).

⁴⁹ corresponding geometric factor $\langle |f_0|^2 f_0^* f_{12} \rangle$ is also an order of magnitude smaller, see G. Lasher, Phys. Rev. **140**, A523 (1965).

⁵⁰ N. Nakai, P. Miranovic, M. Ichioka, and K. Machida, Phys. Rev. Lett. **89**, 237004 (2002).

⁵¹ G. Dresselhaus, A. F. Kip, and C. Kittel, Phys. Rev. **98**, 368 (1955).